Published in Micro & Nano Letters
Received on 28th December 2007
Revised on 25th February 2008
doi: 10.1049/mnl:20070074

ISSN 1750-0443

Properties of graphene produced by the high pressure–high temperature growth process

F. Parvizi[1] *D. Teweldebrhan*[1] *S. Ghosh*[1] *I. Calizo*[1]
A.A. Balandin[1,2] *H. Zhu*[3] *R. Abbaschian*[2,4]

[1]*Nano-Device Laboratory, Department of Electrical Engineering, University of California Riverside, Riverside, CA 92521, USA*
[2]*Materials Science and Engineering Program, Bourns College of Engineering, University of California Riverside, Riverside, CA 92521, USA*
[3]*The Gemesis Corporation, 7040 Professional Parkway East, Sarasota, FL 34240, USA*
[4]*Department of Mechanical Engineering, University of California Riverside, Riverside, CA 92521, USA*
E-mail: balandin@ee.ucr.edu

Abstract: The authors report on a new method for the synthesis of graphene, a mono-layer of carbon atoms arranged in a honey comb lattice, and the assessment of the properties of obtained graphene layers using micro-Raman characterisation. Graphene was produced by a high pressure–high temperature (HPHT) growth process from the natural graphitic source material by utilising the molten Fe–Ni catalysts for dissolution of carbon. The resulting large-area graphene flakes were transferred to the silicon–silicon oxide substrates for the spectroscopic micro-Raman and scanning electron microscopy inspection. The analysis of the *G* peak, *D*, $T + D$ and 2*D* bands in the Raman spectra under the 488 nm laser excitation indicate that the HPHT technique is capable of producing high-quality large-area single-layer graphene with a low defect density. The disorder-induced *D* peak $\sim$1359 cm^{-1} while very strong in the initial graphitic material is completely absent in the graphene layers. The proposed method may lead to a more reliable graphene synthesis and facilitate its purification and chemical doping.

1 Introduction

Recently, the electronic properties of graphene, which is a carbon sheet of a single or few-atomic-layer thickness, attracted much attention owing to its unusual physical properties and the possibility of electronic applications [1–6]. It has been suggested that a band gap can be engineered in a single-layer graphene by spatial confinement [5, 6]. Graphene's extremely high room-temperature carrier mobility makes it a promising material for applications in future nanoelectronic circuits and a number of graphene-based devices have been proposed theoretically or tested [5–10]. It is expected that graphene can be more easily integrated with the standard Si complementary metal-oxide-semiconductor technology than carbon nanotubes owing to graphene's planar geometry. The recently discovered superior thermal conductivity of graphene [11], which exceeds that of carbon nanotubes and diamond, establishes it as a thermal management material and improves its prospects as an electronic material.

To achieve further progress in graphene electronics, one has to develop technology for producing large area, continuous graphene sheets with a controlled number of layers and low defect density. One also has to envision a reliable method for graphene chemical doping. Until now, the highest quality graphene layers were produced by the mechanical exfoliation of graphene from highly oriented pyrolytic graphite (HOPG) with the help of some adhesive such as scotch tape [1]. The process of the peeling of graphene from HOPG pieces is not well-controlled, provides only small size graphene flakes and is difficult to scale up. The reported alternative techniques for producing graphene layers include radio-frequency plasma-enhanced chemical vapour deposition [12], high-vacuum graphene growth by Si sublimation from a 4H-SiC (0001) surface

[13], electrostatic deposition [14], as well as chemical methods [15]. At the same time, the quality of graphene layers produced by the alternative techniques available today is not as good as that of the mechanically exfoliated from HOPG, as evidenced from the low-temperature transport studies and Raman inspection.

2 Method

In this Letter we report on a new approach for producing graphene layers using a high-pressure high-temperature (HPHT) growth process and describe the physical properties of the resulting material. We used the HPHT growth, also referred to as the temperature gradient process [16], to prepare the graphitic material. The samples were synthesised in the split sphere growth apparatus, which is conventionally used for diamond growth [17]. A detailed description of this apparatus has been reported by Abbaschian *et al.* [18]. To produce easily exfoliated graphitic layers we loaded bulk natural graphite on top of the solvent, which was placed on a substrate of stabilised zirconia infiltrated with CsCl (Figs. 1*a*–1*c*). Fig. 1*a* shows a schematic of the chamber and Fig. 1*b* illustrates the growth process. To grow a monocrystal material we used a metal catalyst consisting of Fe–Ni alloy and placed a small seed diamond crystal. During the growth process, the graphite source material completely dissolves in the solvent and re-grows on the substrate as either single- or polycrystalline diamond or graphitic layers, depending on the growth conditions (Fig. 1*b*).

Regardless of the catalyst used, the most critical requirement for producing the desired carbon material is the control of the temperature T and pressure P through the entire process. By varying the growth conditions, we found a regime, which leads to the formation of the loose graphitic layers and flakes of graphene rather than diamond. The selected T and P values were in the range 5–6 GPa and 1300–1700°C, which correspond to the region right below the diamond–graphite equilibrium line in the HPHT phase diagram [18]. Excessive growth rates lead to inclusions and morphological instabilities resulting in strain and high density of defects. For this reason, we kept our mass growth rates low, at about 4 mg/h during the initial stage (less than 40 h), and gradually increased them to about 20 mg/h at the final stage. Such a regime corresponded to an approximately constant deposition rate per unit area (millimetre/hour).

The resulting material, removed from the growth chamber, has a cylindrical shape with ~1 cm diameter and height (Fig. 1*c*). Although most of the cylinder material is of graphitic nature, the bottom re-crystallised carbon layers (up to ~1 mm) are very loosely connected to each other and can be easily peeled off. We have transferred a number of layers to Si/SiO_2 substrates without the help of the adhesives but by simply rubbing the cylinders against the substrates. To confirm the number of layers and assess the quality of HPHT graphene, we used micro-Raman spectroscopy, which has been proven to be the most reliable tool for graphene characterisation [18–24]. It was not possible to carry out micro-Raman characterisation of the top graphene flakes directly on the cylinders, removed from the growth chamber, because of the large background signal from the underlying carbon material. The obtained graphene flakes were large in size with many exceeding ~10 μm in one of the lateral dimensions (Fig. 2*a*). Fig. 2*b* is a scanning electron microscopy (SEM) image of a graphene sample, which was taken to verify the material uniformity.

3 Material characterisation

The micro-Raman spectroscopy was carried out using the confocal Renishaw instrument [21–24]. The spatial

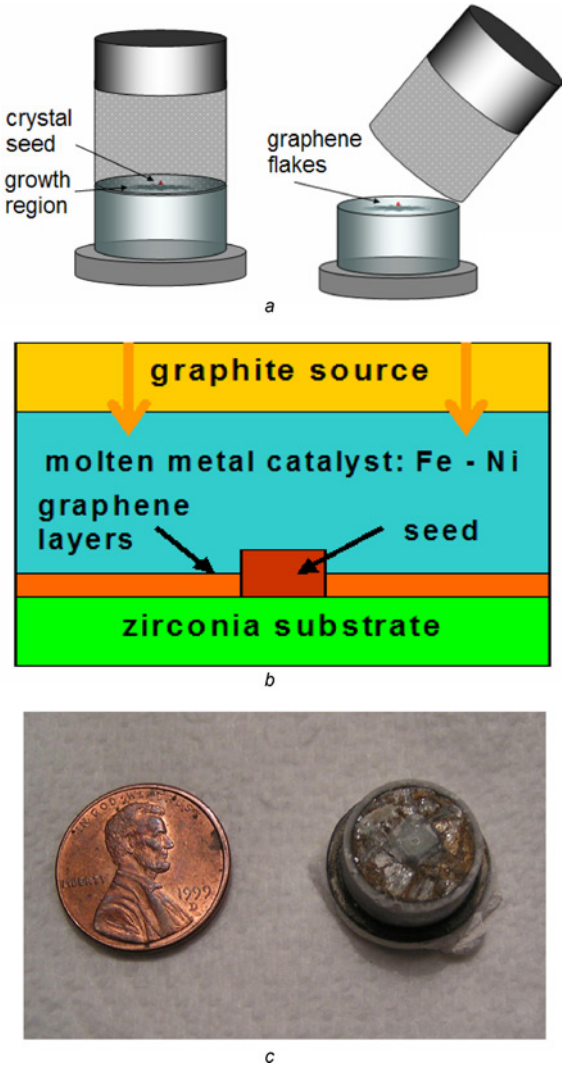

Figure 1 *Schematic and illustration of the growth process and resulting material*

a Schematic of the graphene growth 'cylinder'
b Illustration of the HPHT growth in the 'split sphere' apparatus
c Image of the cylinder with the material after it was removed from the growth chamber
Note that the region in the centre, near the seed, is uniform, indicating crystalline layers, whereas the material at the edges is rough amorphous carbon

doi: 10.1049/mnl:20070074

resolution in our experiments has been limited only by the laser spot size (~1 μm), which allowed us to selectively examine different regions of the few-micrometre-sized graphene layers. The spectra were excited by the 488 nm visible laser and an optical microscope with 50× objective was used to collect the backscattered light. The spectra were recorded with the 1800 lines/mm grating. A special precaution was taken to avoid the local excitation laser heating of the samples by keeping the power on top of the samples below 4 mW.

Figs. 3*a* and 3*b* show a typical spectrum from the HPHT single- and few-layer graphene. The most notable features of the spectrum are the *G* peak at ~1580 cm^{-1}, which corresponds to the E_{2g} mode, and a relatively wide 2*D* band around 2703 cm^{-1} [19–24]. The 2*D* band is an overtone of the disorder-induced *D* band, which is frequently observed in carbon materials at ~1350–1360 cm^{-1}. The *D* band corresponds to the in-plane A_{1g} (LA) zone-edge mode, which is silent for the infinite layer dimensions but becomes Raman active for the small layers or layers with substantial number of defects through the relaxation of the phonon wave–vector selection rules [25]. The band at ~2445 cm^{-1} was attributed to the $T+D_2$ combination similar to the one observed in the carbon-implanted HOPG [26] and graphite crystal edge planes [27]. Although the presence of the *D* band in the spectra taken from the centre of a graphitic sample indicates structural disorder or other defects, this is not the case for the 2*D* band. The second-order phonon 2*D* band is always present in graphene and other carbon materials owing to the double-resonance processes [28] involving two phonons. The arrows in Figs. 2*a* and 2*b* indicate the expected spectral position of the *D* band. The absence of the disorder band in the spectra of HPHT graphene and graphene multilayers confirms the quality of the grown material.

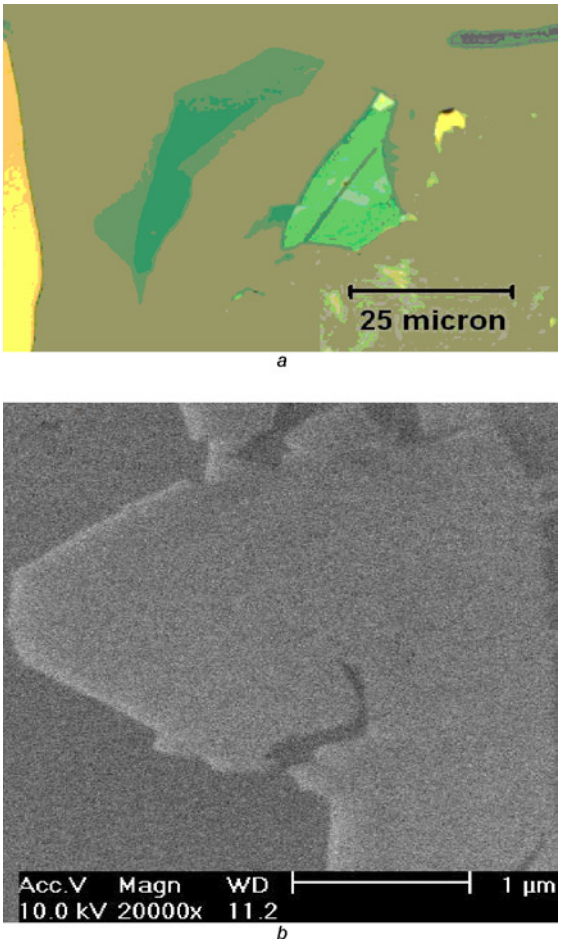

Figure 2 *Microscopic characterisation of HPHT graphene*

a Optical image of the HPHT grown graphene flakes
Grey–green colour regions correspond to single-layer grapheme, and the yellowish regions are bulk graphitic pieces
b SEM image of the edges of a large graphene flake with the dimensions of ~10 × 3 μm^2 produced via the HPHT growth
SEM inspection confirmed the uniformity of graphene layers

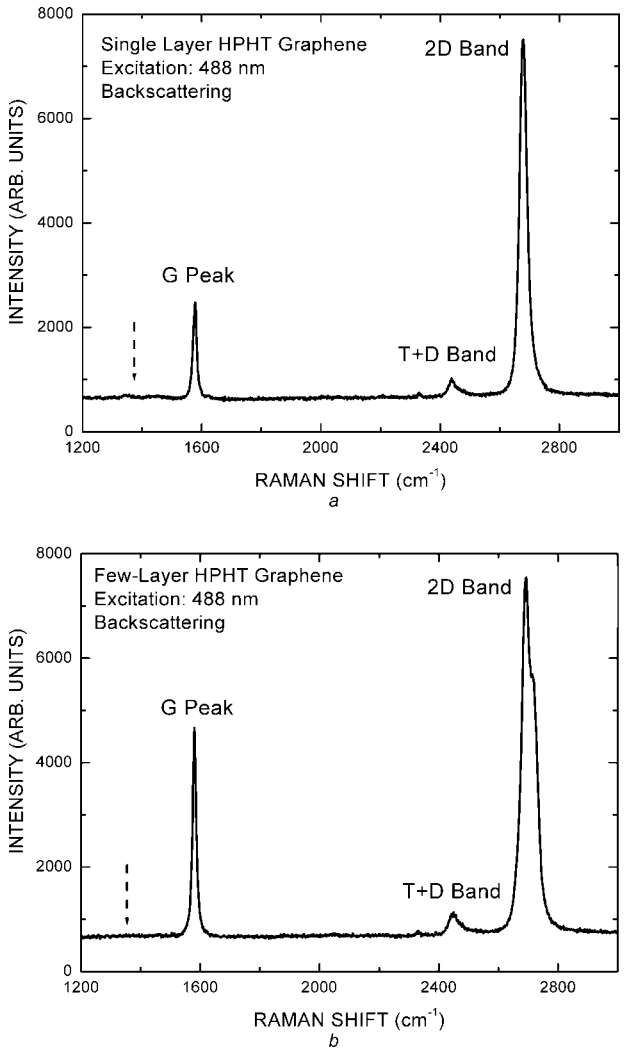

Figure 3 *Raman spectroscopy data for HPHT graphene*

a Single-layer graphene
b Few-layer graphene
Shape and location of the *G* peak and 2*D* band were used to count the layers
Absence of the disorder *D* band near 1350 cm^{-1} attests to the high quality of the grown graphene

To understand the evolution of the material during the HPHT growth process and determine the number of graphene layers, we analysed the *G* peak region and the shape of the 2*D* band in the initial graphite and resulting HPHT material. Fig. 4 shows a close up of the *G* peak region for the initial bulk graphite loaded to the growth apparatus (marked by squares), HPHT as-grown graphitic layers (marked by triangles) and single-layer graphene separated from the top of the HPHT cylinders (marked by circles). The *G* peak position in graphene is slightly up-shifted as compared with graphite, which is in line with Refs. [19–24]. It is interesting to note that the disorder-induced *D* band at 1359 cm^{-1} is very strong in the initial low-grade natural graphite source material but completely absent in as-grown HPHT graphitic layers and single-layer graphene (Fig. 3*a*).

The absence of the *D* band indicates that HPHT graphene has higher crystalline order and lower defect concentration. The latter was attributed to the fact that in HPHT process the carbon is completely dissolved with the help of the molten Fe–Ni catalysts and purified during its transport to a growth site and following re-crystallisation. One should note here that the stage when the carbon is dissolved is suitable for its chemical doping. From the further examination of the figure, one can see that the *G*-peak intensity decrease as one goes from the initial bulk graphite to as-grown HPHT material, and to the single-layer graphene, is expected because of the reduction in the number of the interacting carbon atoms.

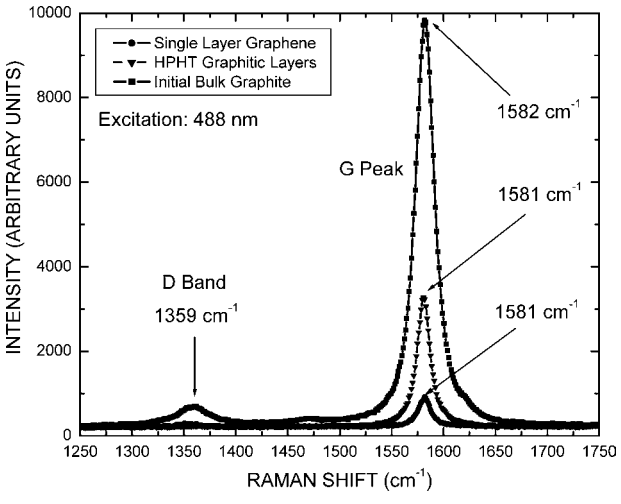

Figure 4 *Raman spectrum of the initial natural bulk graphite source, as-produced HPHT graphitic layers and single-layer graphene in the G-peak region*

Note that the disorder-induced *D* band is very strong in the spectra of the initial bulk graphite and it is completely absent in the spectra of grapheme
This suggests the material quality improves during the growth process via melting and re-crystallisation

Fig. 5 presents a 2*D* band region for the same three forms of the material. Note that while the single-layer graphene signature at 2703 cm^{-1} is a sharp single peak, it is a broader band consisting of two peaks for the initial graphite source and as-grown HPHT graphitic layers. The main 2*D* peak for the initial bulk graphite is located at 2718 cm^{-1}, which exactly corresponds to the doubled frequency of the disorder *D* peak. The second, lower peak, in the initial graphite source and HPHT graphite layers is seen as a shoulder around 2707 cm^{-1}. This observation is in line with the earlier reports that 2*D* peak in bulk graphite consists of the two components $2D_1$ and $2D_2$ [25]. The observed sharp peak in the 2*D* band for the single-layer graphene is in agreement with previously reported data for graphene obtained by the HOPG exfoliation [19–24]. The 2*D* band and *G* peak features confirm that the HPHT produced sample is a single-layer graphene.

To better understand the properties of the graphitic layers grown from the melt via the HPHT process, we carried out thermal conductivity measurements of the HPHT cylinders. The measurements were carried out using the transient planar source 'hot disk' technique [29]. The obtained room temperature cross-plane thermal conductivity is $K \sim 1.3$ W/mK. The typical values reported for the cross-plane thermal conductivity of graphite are between $K = 5.7$ and 40 W/mK [30]. Our result is an average value, which is affected by the presence of zirconia, catalysts and other impurities. The impurities, boundaries and interfaces between layers of different materials are known to reduce the thermal conductivity [31–35]. At the same time, the measured very small value of the thermal conductivity can be an indicator that part of the carbon

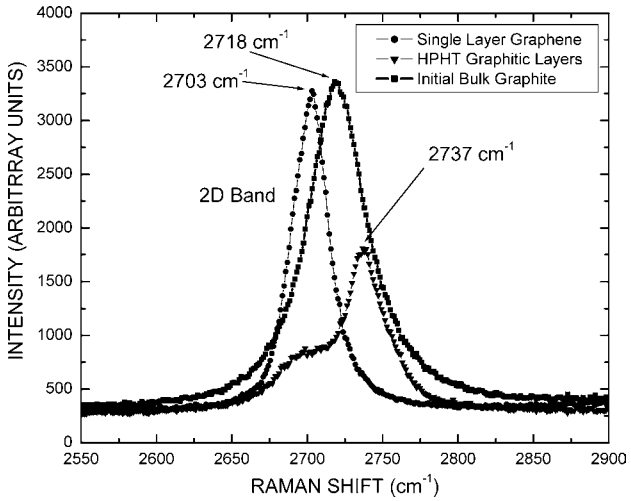

Figure 5 *Raman spectrum of the initial natural bulk graphite source, as-produced HPHT graphitic layers and single-layer graphene in the 2D-band region*

Note that the 2*D*-band from the single-layer graphene is symmetric, whereas those from the bulk graphite and as-produced HPHT manifest a shoulder

doi: 10.1049/mnl:20070074

layers in HPHT are loosely connected, forming the multi-layer graphene flakes. The latter is in line with our observation that the HPHT flakes can be exfoliated very easily.

4 Conclusions

In conclusion, we reported on a new method for the HPHT growth of high-quality large-area graphene layers from the natural graphite. The proposed method may lead to a larger-scale graphene synthesis and a possibility of the efficient purification and chemical doping of graphene during the melt phase of the growth. In the growth process from the natural graphite, we made use of molten Fe–Ni catalysts for the dissolution of carbon. The evolution of the disorder *D* peak as one goes from the initial source carbon to the graphitic layers and then to graphene suggests that the density of the defects reduces and the quality of material improves. The proposed HPHT method may therefore lead to a more reliable graphene synthesis, larger area flakes and facilitate graphene's chemical doping.

5 Acknowledgments

A.A.B. acknowledges support from the DARPA–SRC Focus Center Research Program (FCRP) – Center on Functional Engineered Nano Architectonics (FENA) and the DARPA – DMEA funded UCR – UCLA – UCSB Center for Nanoscience Innovations for Defense (CNID). The authors thank the members of the Nano-Device Laboratory (NDL) for the help with measurements and valuable discussion.

6 References

[1] NOVOSELOV K.S., GEIM A.K., MOROZOV S.V., *ET AL.*: 'Electric field effect in atomically thin carbon films', *Science*, 2004, **306**, pp. 666–669

[2] KHVESHCHENKO D.V.: 'Coulomb-interacting Dirac fermions in disordered graphene', *Phys. Rev. B*, 2006, **74**, p. 161402

[3] DIKIN D.A., STANKOVICH S., ZIMNEY D.J., *ET AL.*: 'Preparation and characterization of graphene oxide paper', *Nature*, 2007, **448**, pp. 457–460

[4] MIAO F., WIJERATNE S., ZHANG Y., COSKUN U.C., BAO W., LAU C.N.: 'Phase-coherent transport in graphene quantum billiards', *Science*, 2007, **317**, pp. 1530–1533

[5] GEIM A.K., NOVOSELOV K.S.: 'The rise of graphene', *Nat. Mater.*, 2007, **6**, pp. 183–191

[6] CASTRO NETO A.H., GUINEA F., PERES N.M.R., NOVOSELOV K.S., GEIM A.K.: 'The electronic properties of graphene', 2007, available at: arXiv:0709.1163v1

[7] GU G., NIE S., FEENSTRA R.M., *ET AL.*: 'Field effect in epitaxial graphene on a silicon carbide substrate', *Appl. Phys. Lett.*, 2007, **90**, p. 253507

[8] HEERSCHE H.B., JARILLO-HERRERO P., OOSTINGA J.B., VANDERSYPEN L.M.K., MORPURGO A.F.: 'Bipolar supercurrent in graphene', *Nature*, 2007, **446**, p. 56

[9] CHO S., CHEN Y.F., FUHRER M.S.: 'Gate-tunable graphene spin valve', *Appl. Phys. Lett.*, 2007, **91**, p. 123105

[10] XU Z., ZHENG Q.S., CHEN G.: 'Elementary building blocks of graphene-nanoribbon-based electronic devices', *Appl. Phys. Lett.*, 2007, **90**, p. 223115

[11] BALANDIN A.A., GHOSH S., BAO W., *ET AL.*: 'Superior thermal conductivity of single-layer graphene', *Nano Lett.*, 2008 doi:10.1021/nl0731872

[12] WANG J.J., ZHU M.Y., OUTLAW R.A., *ET AL.*: 'Free-standing subnanometer graphite sheets', *Appl. Phys. Lett.*, 2004, **85**, p. 1265

[13] HASS J., FENG R., LI T., *ET AL.*: 'Highly ordered graphene for two dimensional electronics', *Appl. Phys. Lett.*, 2006, **89**, p. 143106

[14] SIDOROV A.N., YAZDANPANAH M.M., JALILIAN R., OUSEPH P.J., COHN R.W., SUMANASEKERA G.U.: 'Electrostatic deposition of graphene', *Nanotechnology*, 2007, **18**, p. 135301

[15] HORIUCHI S., GOTOU T., FUJIWARA M., ASAKA T., YOKOSAWA T., MATSUI Y.: 'Single graphene sheet detected in a carbon nanofilm', *Appl. Phys. Lett.*, 2004, **84**, pp. 2403–2405

[16] BUNDY F.P.: 'Direct conversion of graphite to diamond in static pressure apparatus', *Science*, 1962, **137**, pp. 1057–1058

[17] PALYANOV Y.N., MALINOVSKY Y., BORZDOV Y.M., KHOKRYAKOV A.F.: 'Use of the 'split sphere' apparatus for growing large diamond crystals without the use of a hydraulic press', *Dokl. Akad. Nauk SSSR*, 1990, **315**, pp. 233–237

[18] ABBASCHIAN R., ZHU H., CLARKE C.: 'High pressure–high temperature growth of diamond crystals using split sphere apparatus', *Diam. Relat. Mater.*, 2005, **14**, pp. 1916–1919

[19] FERRARI A.C., MEYER J.C., SCARDACI V., *ET AL.*: 'Raman spectrum of graphene and graphene layers', *Phys. Rev. Lett.*, 2006, **97**, p. 187401

[20] GUPTA A., CHEN G., JOSHI P., TADIGADAPA S., EKLUND P.C.: 'Raman scattering from high-frequency phonons in supported n-graphene layer films', *Nano Lett.*, 2006, **6**, pp. 2667–2673

[21] CALIZO I., BALANDIN A.A., BAOW, MIAO F., LAU C.N.: 'Temperature dependence of the Raman spectra of graphene and graphene multilayers', *Nano Lett.*, 2007, **7**, (9), pp. 2645–2649

[22] CALIZO I., MIAO F., BAO W., LAU C.N., BALANDIN A.A.: 'Variable temperature Raman microscopy as a nanometrology tool for graphene layers and graphene-based devices', *Appl. Phys. Lett.*, 2007, **91**, p. 071913

[23] CALIZO I., BAO W, MIAO F., LAU C.N., BALANDIN A.A.: 'Graphene-on-sapphire and graphene-on-glass: Raman spectroscopy study', *Appl. Phys. Lett.*, 2007, **91**, p. 201904

[24] CALIZO I., TEWELDEBRHAN D., BAO W., MIAO F., LAU C.N., BALANDIN A.A.: *J. Phys. C.*, 2008 (in press)

[25] VIDANO R.P., FISCHBACH D.B., WILLIS L.J., LOEHR T.M.: 'Observation of Raman band shifting with excitation wavelength for carbons and graphites', *Solid State Commun.*, 1981, **39**, p. 341

[26] TAN P.H., DENG Y.M., ZHAO Q.: 'Temperature-dependent Raman spectra and anomalous Raman phenomenon of high oriented pyrolytic graphite', *Phys. Rev. B*, 1998, **58**, pp. 5435–5439

[27] TAN P.H., DIMOVSKI S., GOGOTSI Y.: 'Raman scattering of non-planar graphite: arched edges', *Phil. Trans. R. Soc. Lond. A*, 2004, **362**, pp. 2289–2310

[28] THOMSEN C., REICH S.: 'Double resonant Raman scattering in graphite', *Phys. Rev. Lett.*, 2000, **85**, pp. 5214–5217

[29] GUSTAFSSON S.E.: 'Transient plane source techniques for thermal conductivity and thermal diffusivity measurements of solid materials', *Rev. Sci. Instrum.*, 1991, **62**, p. 797

[30] YU C., SAHA S., ZHOU J., *ET AL*.: 'Thermal contact resistance and thermal conductivity of a carbon nanofiber', *Trans. ASME*, 2006, **128**, p. 234

[31] SHAMSA M., LIU W.L., BALANDIN A.A., CASIRAGHI C., MILNE W.I., FERRARI A.C.: 'Thermal conductivity of diamond-like carbon films', *Appl. Phys. Lett.*, 2006, **89**, p. 161921

[32] LIU W.L., SHAMSA M., CALIZO I., *ET AL*.: 'Thermal conduction in nanocrystalline diamond films: Effects of the grain boundary scattering and nitrogen doping', *Appl. Phys. Lett.*, 2006, **89**, p. 171915

[33] LIU W.L., BALANDIN A.A.: 'Thermal conduction in AlGaN alloys and thin films', *J. Appl. Phys.*, 2005, **97**, p. 073710

[34] ZOU J., KOTCHETKOV D., BALANDIN A.A.: 'Thermal conductivity of GaN films: effects of impurities and dislocations', *J. Appl. Phys.*, 2002, **92**, pp. 2534–2539

[35] KOTCHETKOV D., ZOU J., BALANDIN A.A., FLORESCU D.I., POLLAK F.H.: 'Effect of dislocations on thermal conductivity of GaN layers', *Appl. Phys. Lett.*, 2001, **79**, pp. 4316–4318

doi: 10.1049/mnl:20070074